

# Properties of barium hexaferrite thick films deposited by electron beam evaporation

M. Vérité\*, M. Valetas, A. Bessadou, F. Cosset, J.C. Vareille

*IRCOM Laboratory (UMR 6615)/Equipe Composants et Circuits Micro-Électroniques et Micro-Optiques,  
123, Avenue Albert Thomas—87060 Limoges Cedex, France*

Received 8 December 2003; received in revised form 11 March 2004; accepted 21 March 2004  
Available online 11 November 2004

## Abstract

This paper presents results obtained on barium ferrite thick films prepared by electron beam evaporation. First of all, we have looked at the influence of substrate temperature on the films properties. Then, we have fixed the substrate temperature to 700 °C and the effects of films thickness on the different properties has been investigated. Indeed for a substrate temperature of 700 °C we have observed that the layers are crystallized in the BaM phase with in-plane preferential orientation. However, a secondary non magnetic phase ( $\text{BaFe}_2\text{O}_4$ ), which can modify the magnetic properties, appears on some layers.

© 2004 Elsevier Ltd. All rights reserved.

*Keywords:* Ferrites; Films; Microwave devices; X-ray methods; Magnetic properties;  $\text{BaFe}_{12}\text{O}_{19}$

## 1. Introduction

The emergence of mobile communications in recent years has revitalized the study of new ferrite devices and their applications based on the non-reciprocal property of these materials. Currently, non-reciprocal systems, such as circulators, use bulk ferrites. This component can be used in duplex communication systems to separate the incoming and outgoing waves. The specification of such devices are detailed in the paper of Martha Pardavi-Horvarth.<sup>1</sup>

The increase of working frequency leads to a decrease of the ferrite junction diameter. Indeed, this parameter must be equal to the half guided wavelength. In our laboratory, we have focused our researches on the realization of an integrated circulator working at 77 GHz, which is a working frequency for military applications. But at this frequency, a paper published by Denis C. WEBB explains that the films must have a thickness at least equal to 50  $\mu\text{m}$  to minimize insertion losses in the circulator<sup>2</sup> (Fig. 1). Such thicknesses cannot be reached by machining a bulk material. Consequently, it is necessary to use materials under film forms ob-

tained with a fast deposition technique: electron beam evaporation.

In this paper we present the results obtained on thick barium hexaferrite films. The strong anisotropy and high coercivity of M-type barium hexaferrite ( $\text{BaFe}_{12}\text{O}_{19}$ ), along with their chemical and mechanical stability make them a very important class of materials for microwaves and high density magnetic and magneto-optical technologies.<sup>3</sup>

To increase adhesion and minimize cracks, the ferrite films are grown on gold on titanium underlayers realized on Silicon (100) substrates. The metallic layers, which are deposited by dc cathodic magnetron sputtering, will also play the role of ground plane in the circulator design.

This work deals with the influence of the deposition parameters (substrates temperature and thickness) on films properties (crystallographic and magnetic properties, morphology, composition). A previous study concerning the influence of the deposition rate has already been published.<sup>4</sup>

## 2. Experimental procedure

Before deposition, the substrates are cleaned by  $\text{Ar}^+$  bombardment using an RF generator in the following conditions:

\* Corresponding author. Tel.: +33-5-55-45-74-48;

fax: +33-5-55-45-74-50.

E-mail address: [marc.verite@unilim.fr](mailto:marc.verite@unilim.fr) (M. Vérité).

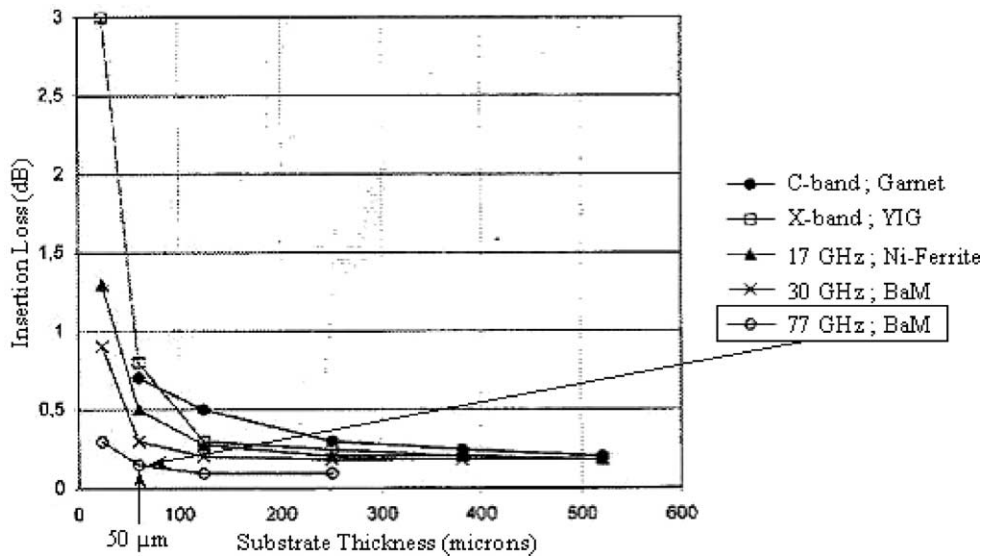


Fig. 1. Circulator insertion loss as a function of substrate thickness for several material–frequency combinations.<sup>2</sup>

- argon pressure: 0.33 Pa, RF incident power: 200 W, cleaning time: 5 min.

Then the ferrite ( $\text{BaFe}_{12}\text{O}_{19}$ ) is evaporated under 100% oxygen atmosphere with a total deposition pressure of 0.46 Pa.

The post-annealing procedure is realized under the following conditions:

- annealing temperature: 850 °C, oxygen pressure:  $5 \times 10^4$  Pa, annealing time: 2 h, rise time: 10 °C/min.

The crystallographic structure is analyzed by X-ray diffraction (XRD) with a SIEMENS generator equipped with a goniometer. The saturation magnetization intensity ( $J_s$ ) and coercive field ( $H_c$ ) are measured using a hysteresisometer M2100 with alternative magnetic field (50 Hz) applied in the film plane. We use a scanning electron microscope (SEM) equipped with an energy dispersive X-ray (EDX) analysis system to characterize morphology and to determine stoichiometric ratio. Finally, Secondary Ion Mass

Spectrometry (SIMS) is used to realize depth concentration profiles.

### 3. Experimental results

#### 3.1. Structural properties

We have studied the influence of substrates temperature on the crystallographic properties for two deposition rates (10 and 20  $\mu\text{m}/\text{h}$ ). In these case, the layers have a thickness close to 20  $\mu\text{m}$ .

Fig. 2 shows that, for a deposition rate of 10  $\mu\text{m}/\text{h}$ , when the substrate temperature is lower than 700 °C, the films are amorphous or with poor crystallization. Indeed, the most important diffraction peaks are those of metallic underlayers (gold on titanium). We also observe the formation of a secondary phase  $\text{BaFe}_2\text{O}_4$ . This phenomenon may be explained by the fact that the films are not stoichiometric ( $\text{Fe}/\text{Ba} \neq$

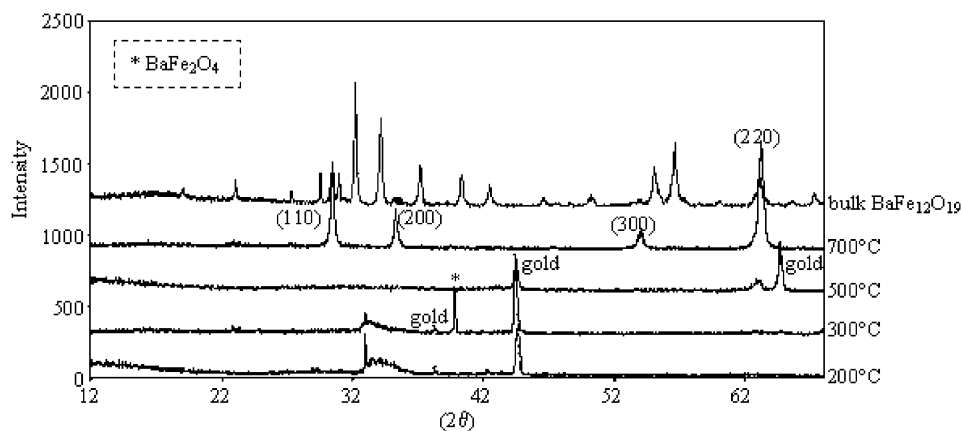


Fig. 2. XRD patterns of films realized at different substrate temperature for a deposition rate of 10  $\mu\text{m}/\text{h}$ .

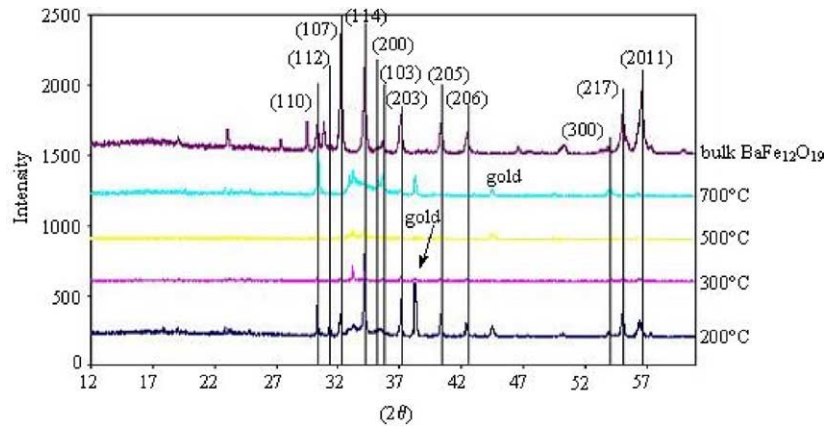


Fig. 3. XRD patterns of annealed films realized at different substrate temperature for a deposition rate of 20  $\mu\text{m/h}$ .

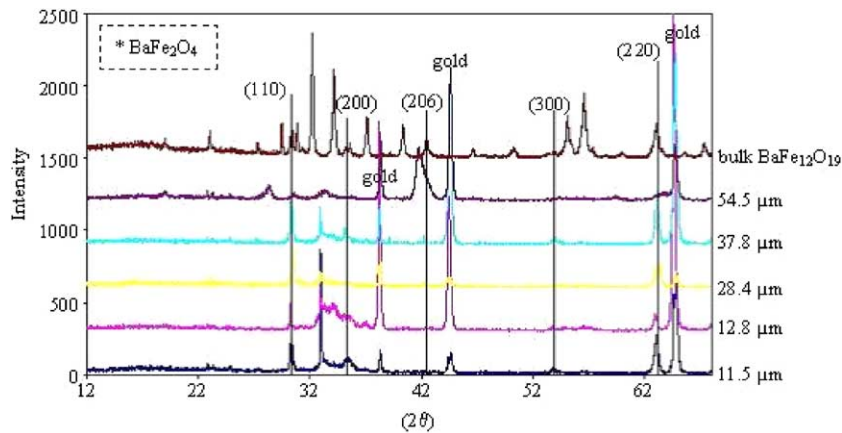


Fig. 4. XRD patterns of films realized with different thicknesses ( $T_s = 700^\circ\text{C}$ ).

12).<sup>5</sup> When the substrate temperature is equal to 700 °C the films are crystallized with in plane preferential orientation (1 1 0) and (2 2 0). After annealing all the films are crystallized mainly according to the M-BaFe<sub>12</sub>O<sub>19</sub> phase. The layers exhibit in plane preferential orientation for a deposition temperature of 700 °C and are not oriented for lower deposition temperatures.

For a deposition rate of 20  $\mu\text{m/h}$  the results are similar (Fig. 3).

In a previous study, we have observed that the iron on barium ratio is closed to 12 when the deposition rate is equal to 30  $\mu\text{m/h}$ .<sup>4</sup> So we have studied the evolution of the crystallographic properties as a function of films thickness for a substrate temperature of 700 °C and a deposition rate close to 30  $\mu\text{m/h}$ . We observe in Fig. 4 that the films present in plane preferential orientation and the secondary phase (BaFe<sub>2</sub>O<sub>4</sub>) appears for a thickness of 54.5  $\mu\text{m}$ . This phenomenon is observed for smaller thicknesses when deposition rate decreases. Indeed, for a deposition rate of 17  $\mu\text{m/h}$  the phase mixing appears for a thickness close to 36  $\mu\text{m}$ .

### 3.2. Magnetic properties

For temperatures lower than 700 °C the films are amorphous, so the magnetic properties are mainly measured on annealed samples. In Fig. 5 is plotted the evolution of coercive field against substrate temperature for the two deposition rates previously studied (10 and 20  $\mu\text{m/h}$ ). We observe that  $H_c$  decreases when substrate temperature increases.

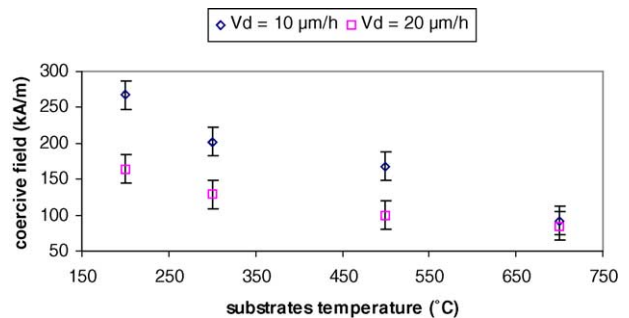


Fig. 5. Evolution of coercive field against substrate temperature for two deposition rates.

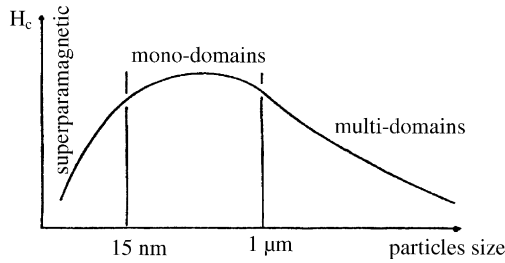


Fig. 6. Evolution of coercive field against particles size.

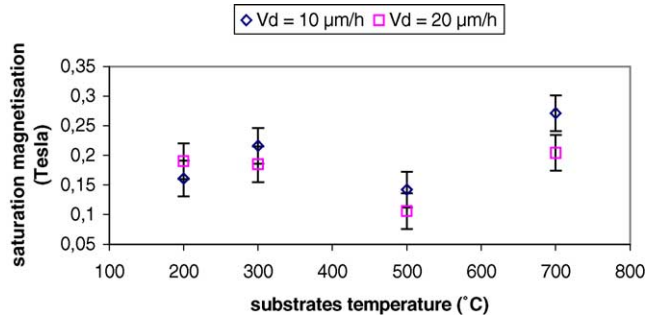


Fig. 7. Evolution of saturation magnetisation against substrate temperature for two deposition rates.

Indeed, it varies between 267 and 92 kA/m and between 164 and 85 kA/m when the deposition rate is respectively equal to 10 and 20 μm/h. This phenomenon can be explained by the Movchan and Demchishin (M–D) diagram<sup>6</sup> and by the fact that the grains are multi-domains. Indeed, on the one hand, during the deposition, the M–D diagram shows that when substrate temperature increases grains size increases. On the other hand, the measured grains size is always higher than 1 μm. In this case, as shown on Fig. 6, we are in a multi-domains configuration, and larger is the grains size lower is the coercive field.<sup>7</sup>

Moreover, from Fig. 7 it is very difficult to deduce a specific influence of substrate temperature or deposition rate on the saturation magnetization. Indeed, it varies from 0.11 to 0.22 T. We can note that the maximum value is less than the 0.4 T of the bulk material. It probably results from the formation of a non magnetic buffer layer between ferrite film and substrate during the annealing procedure.<sup>8</sup> It can also be due to the presence of the non-magnetic phase: BaFe<sub>2</sub>O<sub>4</sub>.<sup>9</sup>

Fig. 8 represents the evolution of coercive field against films thickness before and after annealing. During this study the layers are realized with a substrates temperature of 700 °C, a deposition rate close to 30 μm/h and the thickness varies from 11 to 54.5 μm. Before annealing, H<sub>c</sub>

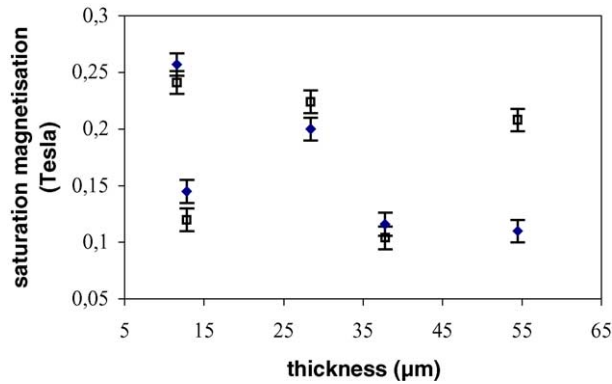


Fig. 8. Variation in coercive field as a function of films thickness.

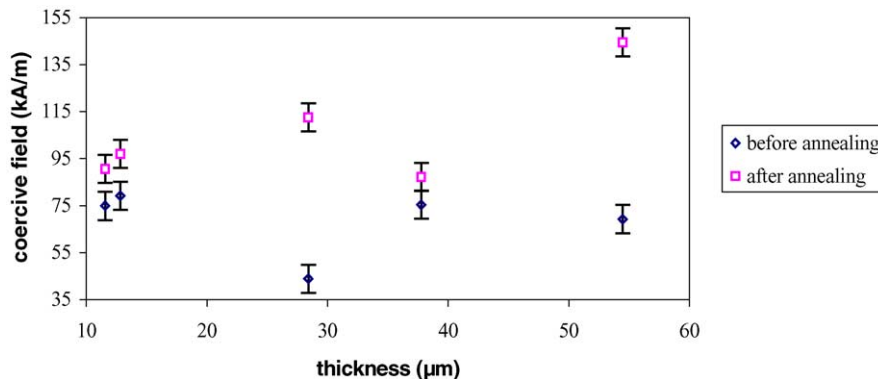


Fig. 9. Variation in saturation magnetisation as a function of thickness.

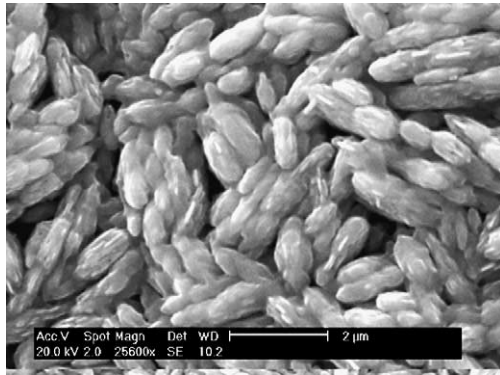


Fig. 10. SEM picture of a film realized at a substrate temperature of 700 °C.

is constant and closed to 69 kA/m. This result has already been observed for thin layers ( $8 \text{ nm} < \text{thickness} < 100 \text{ nm}$ ) deposited by Facing Target Sputtering,<sup>10</sup> but in this case the measured values were lower ( $H_c \approx 24 \text{ kA/m}$ ). After annealing  $H_c$  increases and varies between 87 and 144 kA/m. The evolution of saturation magnetization against films thickness is plotted in Fig. 9. We see that the saturation magnetization varies between 0.1 and 0.26 T before annealing. After annealing, for thicknesses lower than 54.5  $\mu\text{m}$  the measured values are identical. At 54.5  $\mu\text{m}$  the saturation magnetization increases and reaches a value of 0.2 T.

#### 4. SEM and EDX properties

The SEM micrograph of the film prepared at a substrate temperature of 700 °C is shown in Fig. 10. It confirms the X-ray diffraction results. Indeed, the picture shows a mosaic of rod-like particles with sharp ends, whose long axis is randomly distributed within the plane of the film.<sup>11</sup>

Table 1

Evolution of Fe/Ba as function of the substrate temperature

	Temperature (°C)			
	200	300	500	700
Fe/Ba ( $V_d \approx 10 \mu\text{m/h}$ )	7.6	7.7	10.6	12.6
Fe/Ba ( $V_d \approx 20 \mu\text{m/h}$ )	11.1	26.7	17.8	14.6

Table 1 presents the evolution of the Fe/Ba ratio against substrate temperature for two deposition rates (10 and 20  $\mu\text{m/h}$ ). For 10  $\mu\text{m/h}$  the iron on barium ratio increases when substrate temperature increases. For a higher deposition rate (20  $\mu\text{m/h}$ ) we cannot deduce any specific influence of substrate temperature. In this case, the evolution observed for a deposition rate of 10  $\mu\text{m/h}$  may be masked by the existence of a vapor cloud above the ingot surface.<sup>12</sup>

When the thickness increases the Fe/Ba ratio decreases before and after annealing. We must note that after annealing the measured values are higher than before annealing. It is probably caused by a diffusion of barium during the procedure of annealing.

The fact that the iron on barium ratio decreases with increasing thickness highlights a preferential evaporation phenomenon. Indeed, the iron oxide is first evaporated because of its evaporation temperature (1565 °C at  $10^5 \text{ Pa}$ ) which is lower than the evaporation temperature of barium oxide (1923 °C at  $10^5 \text{ Pa}$ ). To confirm this result we have realized a SIMS depth profile (Fig. 11) on a layer having a thickness closed to 54.5  $\mu\text{m}$ . It shows that the film composition is not homogeneous which confirms previous hypothesis. Other coatings have been realized with a different thickness and for two deposition rates: 5 and 17  $\mu\text{m/h}$ . Results are presented in Fig. 12. The observed evolutions are identical. Indeed, the Fe/Ba ratio decreases with increasing thickness. It varies between 7.4 and 24.7 for a deposition rate close to

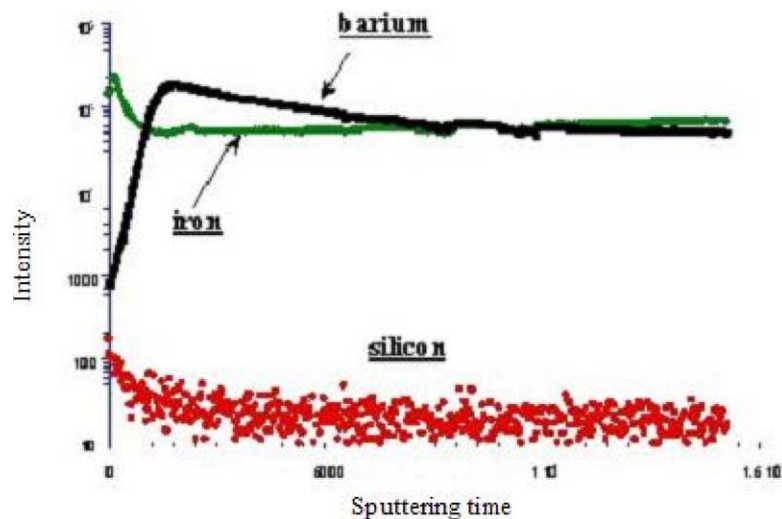


Fig. 11. SIMS depth profile for a thickness layer closed to 54.5  $\mu\text{m}$ .

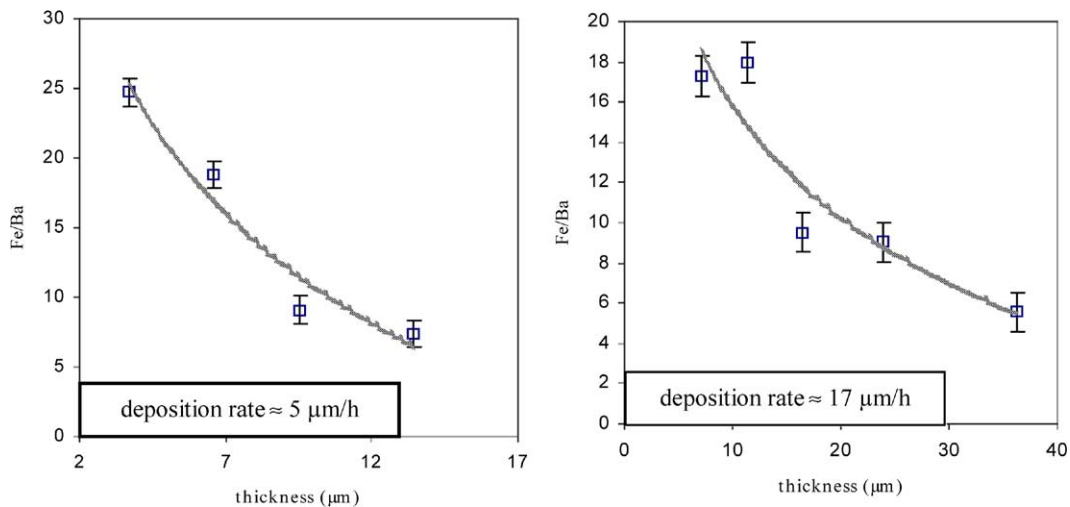


Fig. 12. Evolution of Fe/Ba ratio against films thickness.

5  $\mu\text{m/h}$  and between 5.6 and 17.9 for a deposition rate of 17  $\mu\text{m/h}$ .

## 5. Conclusion and discussion

In conclusion, we have emphasized a preferential evaporation phenomenon during the evaporation process. Moreover, chemical analysis has shown that the ingot composition has already changed during its formation (see Table 2). This problem will be solved by the use of a twin beam evaporation system. Indeed, iron oxide and barium oxide, which have different evaporation temperatures, will be evaporated separately and the films stoichiometric ratio will be controlled by adjusting each beam power. Results will be published in the next paper.

Moreover, the magnetic properties obtained here are acceptable for the realization of an integrated circulator working at 77 GHz<sup>3</sup> but for this application we have to obtain a crystallographic orientation perpendicular to the film plane. One possible solution consists in applying a magnetic field perpendicular to the film plane during the evaporation process.<sup>13</sup> Another one consists in modifying the substrate nature (Si(1 1 1) or Al<sub>2</sub>O<sub>3</sub>(0 0 0 1)) in order to adapt lattice parameters between the substrate and the layer. Some attempts are currently in progress and results will be published in the next paper.

In all cases, we have obtained pure BaFe<sub>12</sub>O<sub>19</sub> phase or a phase mixing: BaFe<sub>12</sub>O<sub>19</sub> + BaFe<sub>2</sub>O<sub>4</sub> depending on the evaporation conditions.

Another means to realize the junction, studied in our group, consists in using a soft ferrite film biased with a per-

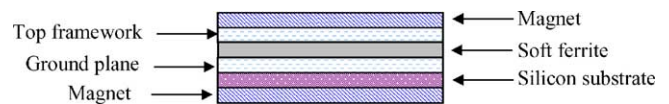


Fig. 13. Circulator junction using a soft ferrite biased with a permanent magnet.

manent magnet (SmCo<sub>5</sub> or Nd<sub>2</sub>Fe<sub>14</sub>B) showing the good orientation. In this case, one representation of this device is shown in Fig. 13. Si/Ti/NdFeB/Ti multilayers have been prepared by RF magnetron sputtering and promising results have been obtained.<sup>14</sup>

## References

1. M. Pardavi-Horvath, Microwave applications of soft ferrites, *J. Magn. Mater.* 215/216 (2000) 171–183.
2. Webb, D. C., Design and fabrication of low-cost ferrite circulators. In *Proceedings of the 25th European Microwave Conference, Bologna, Italy, 4–7 September 1995*. pp. 1191–1197.
3. M. Koleva, et al. Pulsed laser deposition of barium hexaferrite (BaFe<sub>12</sub>O<sub>19</sub>) thin films, *Appl. Surf. Sci.* 154–155 (2000) 485–491.
4. M. Vérité, et al. The study of barium ferrite thick films prepared by electron beam evaporation, *J. Eur. Ceram. Soc.* 21 (2001) 1925–1929.
5. G. Mendoza-Suarez, et al. Influence of stoichiometry and heat treatment conditions on the magnetic properties and phase constitution of Ba-ferrite powders prepared by sol–gel, *Mater. Chem. Phys.* 9454 (2002) 1–6.
6. Richardt, A. and Durand, A. M., *Le vide, Les couches minces, Les couches dures*, Editions IN FINE, 1994, pp. 280–281.
7. Sarda, C., Contribution à l'étude de l'hexaferrite de baryum et des ferrites spinelles dopée au baryum. *Application à l'enregistrement magnétique*. Thèse de doctorat en Sciences des matériaux, Université Paul Sabatier de Toulouse, mai 1993, p. 19.
8. X. Liu, et al. The study of sputtered Barium ferrite thin films, *Phys. Stat. Sol.* 174 (1999) 389.
9. G. Mendoza-Suarez, et al. Magnetic properties and microstructure of Ba-ferrite powders prepared by ball milling, *J. Magn. Mater.* 223 (2001) 55–62.
10. S. Nakagawa, N. Matsushita, M. Naoe, et al. Perpendicular magnetic recording media using hexagonal ferrite thin films deposited on Pt

Table 2  
Chemical analysis of an ingot after fusion

Ba (%)	Fe (%)	Fe/Ba
17.29	58.81	8.38

- underlayers and interlayers, *J. Magn. Magn. Mater.* 235 (2001) 337–341.
11. Zhang X. Y. et al, Barium ferrite films with in-plane orientation grown on silicon by pulsed laser deposition 1998, **190**, 171–175.
  12. Malaurie, A., *Modélisation des mécanismes de transport de la vapeur métallique dans les techniques de dépôt physique en phase vapeur*. Thèse de doctorat en matériaux céramiques et traitements de surface, Université de Limoges, janvier 1995, pp. 11–12.
  13. Ji, Z. G., Copper phthalocyanine film grown by vacuum deposition under magnetic field. *Thin Solid Films*, 2002, **402**, 79–82.
  14. Valetas, M., *Couches minces magnétiques pour applications hyperfréquences: étude des Samarium-Cobalt et Néodyme-Fer-Bore par pulvérisation radiofréquence magnétron*. Thèse de doctorat Electronique des hautes fréquences et Optoélectronique, Université de Limoges, novembre 2003.